Repetitive Firing: Quantitative Analysis of Encoder Behavior of Slowly Adapting Stretch Receptor of Crayfish and Eccentric Cell of *Limulus*

J. F. FOHLMEISTER, R. E. POPPELE, and R. L. PURPLE

From the Laboratory of Neurophysiology, University of Minnesota, Minneapolis, Minnesota 55455

ABSTRACT Techniques developed for determining summed encoder feedback in conjunction with the leaky integrator and variable-γ models for repetitive firing are applied to spike train data obtained from the slowly adapting crustacean stretch receptor and the eccentric cell of *Limulus*. Input stimuli were intracellularly applied currents. Analysis of data from cells stringently selected by reproducibility criteria gave a consistent picture for the dynamics of repetitive firing. The variable-γ model with appropriate summed feedback was most accurate for describing encoding behavior of both cell types. The leaky integrator model, while useful for determining summed feedback parameters, was inadequate to account for underlying mechanisms of encoder activity. For the stretch receptor, two summed feedback processes were detected: one had a short time constant; the other, a long one. Appropriate tests indicated that the short time constant effect was from an electrogenic sodium pump, and the same is presumed for the long time constant summed feedback. Both feedbacks show seasonal and/or species variations. Short hyperpolarizing pulses inhibited the feedback from the long time constant process. The eccentric cell also showed two summed feedback processes: one is due to self inhibition, the other is postulated to be a short time constant electrogenic sodium pump similar to that described in the stretch receptor.

INTRODUCTION

In the previous paper (Fohlmeister et al., 1977), we established a theoretical framework for dealing with encoder feedback in the context of well-defined models. Now we shall apply the techniques developed to formulate a description of nerve impulse encoder operation for two repetitively firing sensory neurons.

Previous work on the slowly adapting stretch receptor of crayfish was led to the hypothesis that there is an electrogenic Na^+ pump which responds to increments of Na^+ that enter the cell with each action potential (Nakajima and Takahashi, 1966; Sokolove and Cooke, 1971). Such a mechanism might be expected to produce a summed feedback of the kind discussed in the companion paper. We will show here evidence based on spike train analysis and simulation that is consistent with that hypothesis. In addition, the *Limulus* eccentric cell is a

well-documented example of a neuron having synaptic inhibitory feedback in the form of self-inhibition (Purple, 1964). Each action potential produced by the cell leads to an inhibitory postsynaptic potential in the same cell. Therefore, it represents another case of a neuron with spike-locked summed feedback.

Analysis of the responses of these cells to intracellularly applied constant current, step current, and small amplitude sinusoidally modulated current leads to a consistent picture of the dynamics of their repetitive firing behavior. The variable-γ model (Fohlmeister, 1973) with the addition of appropriate summed feedback is sufficient to account for steady-state and dynamic responses in both cells.

MATERIALS AND METHODS

Impulse activity was evoked in slowly adapting stretch receptors of the crayfish and the eccentric cell from the lateral eye of *Limulus* by intracellularly applied current. Data are reviewed here from 21 stretch receptors of the crayfish *Cambarus astacus* and *Procambarus clarki*, and from nine eccentric cells of the lateral eye of *Limulus polyphemus*. The units were selected from a total of more than 100 impaled crayfish receptors and from a lesser number (around 50) of eccentric cells. They yielded the most accurate data obtained from cells of the total population studied, and they met stringent criteria for stability and longevity in conjunction with stability of the impaling micropipette. Thus the units reported on here may be exceptional in terms of the accuracy of data elicited from them, but they were not biologically atypical. Virtually all other units studied yielded similar though less accurate results.

Crayfish Stretch Receptors

Isolated slowly adapting stretch receptors from abdominal segments of the crayfish were placed in modified van Harreveld's solution (Fohlmeister et al., 1974). For *C. astacus* (Mogul-Ed, Inc., Wisconsin), the basic solution contained 205 mM NaCl, 5 mM KCl, 12 mM $CaCl_2$, 2.6 mM $MgCl_2$, and 5 mM Tris buffer with pH adjusted to 7.5 at 15°C. From October to February of each year, the sodium content of the solution was dropped to 160 meq and calcium was elevated to 14 meq since these animals gain extracellular calcium and lose extracellular sodium during the winter (Drilhon-Courtois, 1934). For *P. clarki* (Carolina Biological Supply Co., Burlington, N. C.), the basic solution was 160 mM NaCl, 5.6 mM KCl, 12.2 mM $CaCl_2$, 2 mM $MgCl_2$, and 5 mM Tris buffer adjusted to pH 7.5 at 15°C.

Isolated receptors were mounted in a 2-cm^3 lucite perfusion chamber. Ends of the tonic muscle were tied with fine threads which were clamped by forceps mounted on a manipulator to provide for either symmetrical or asymmetrical stretches. Temperature was generally maintained at 15° ± 0.5°C by a Peltier-effect cooling device driven by a thermoregulatory circuit whose thermistor probe was mounted within the chamber. Impulse activity was recorded both by a suction electrode on the axon and by intracellular recording with either 0.5 M K-citrate or 3.0 M KCl-filled micropipettes. The intracellular recording equipment, including an active bridge circuit for measuring cell and micropipette resistances has been described (Purple, 1964; Fohlmeister et al., 1974). Micropipette resistances were between 15 and 25 MΩ. Two stability requirements for each experiment were that pipette resistances did not increase by more than 5 MΩ during the course of the intracellular experiments, and that the pipette's capability to pass currents up to 5 nA without rectifying by more than 1 MΩ be maintained throughout the duration of the impalement.

After each cell had been tested for its ability to produce repetitive trains at different

levels of stretch, the cell was impaled and the muscle bundle was then relaxed so that the cell's dendritic complex and the muscle bundle were slack. This procedure helped to insure that current from the intracellular pipette represented the only source of drive to the cell's trigger zone. All the cells selected (except those subjected to K-free conditions) remained in stable condition for at least 4 h after impalement. Stability limits were: (*a*) the resting potential in normal perfusate remained within ±2 mV of the value measured at the start of data acquisition; (*b*) resting cell resistance remained within ±0.6 MΩ of the initial value; (*c*) membrane rectification to depolarizing currents of up to 5 nA did not show resistance decreases of more than 1–1.5 MΩ, and this property remained constant for the duration of the experiment; and (*d*) the impaled units remained capable of sustained repetitive impulse trains of 15 imp/s or more to applied current that lasted for 2 min. This last property was also checked for the constancy of current required to produce firing at 15 imp/s. The criteria for cell stability coupled with those for micropipette stability, while stringent enough to exclude data from most of the units impaled, were sufficient when met to allow for a reproducibility of data that was significant to within 0.5 dB or better in amplitude measurements (i.e. ±6%) and to within ±3° in phase measurements. Fig. 1 and the accompanying Table 1 illustrate this point. Fig. 1 is a Bode plot of gain and phase (see Fohlmeister et al., 1977) of the output impulse train showing three separate frequency modulation runs during which six separate pairs of gain and phase parameters were accumulated for two runs and four pairs for the third run. For each point of gain and phase data, at least 30 s of sustained, repetitive impulse activity (200 or more impulses) was sampled. 0.5 h separated each of the three runs.

When the perfusate was changed by addition of ouabain, or by altering or removing extracellular potassium, data taking was performed under conditions of continuous perfusion (0.2 cm^3/min) to insure that the perfusate remained fresh and unaltered. In normal perfusate, no differences were observed between continuous perfusion conditions and conditions of no flow.

The most fragile part of the cell machinery appears to be that responsible for sustained repetitive firing. Often a tonic unit would become phasic, or would lose its ability to fire at all, although stretch-induced generator potentials still appeared normal and cell resistance and resting potentials changed very little. Attempts to abolish the electrogenic sodium pump, for instance by substituting lithium for sodium (unpublished experiments), resulted in a rapid decline in the capability of impaled cells to sustain repetitive trains for several minutes, and this property did not recover despite repeated and prolonged attempts at reperfusing in normal solutions. The effect of lithium on the generator potential was, however, quite reversible (cf. Obara and Grundfest, 1968). Similarly potassium-free solutions usually had a rapid, irreversible effect on a cell's ability to sustain repetitive impulse trains. Only on three occasions were we successful in reversing (incompletely at that) effects of preparations maintained in K-free solution for the 30–60 min required to complete data taking for one Bode plot. This behavior of the repetitive firing machinery in-K-free solutions can be contrasted to the much more reversible effects on the generator potential (Edwards et al., 1963) and on the ability of the axon to conduct propagated impulses after relatively short exposures (Sokolove and Cooke, 1971). Similar findings were made for the eccentric cells in *Limulus*, although these units could withstand considerable periods in low (not zero) potassium solutions with complete reversibility of the sustained firing characteristics if sufficient recovery time (at least 30 min) was allowed in the normal perfusate.

Eccentric Cells

Thin slices (Purple, 1964; Adolph, 1976) of the lateral eye were placed in a lucite perfusion chamber whose volume was 1.5 cm^3. The normal perfusate contained 420 mM NaCl, 10

mM KCl, 6.3 mM$MgSO_4$, 18.7 mM $MgCl_2$, 10 mM $CaCl_2$, and 10 mM Tris buffer, with the pH adjusted to 7.6. In solutions of altered potassium, NaCl was added or subtracted as needed to insure a constant osmolarity. The thin slices were illuminated at a low background intensity (ca. 0.15–0.2 cd/m²) to partially suppress the amplitudes of the slow

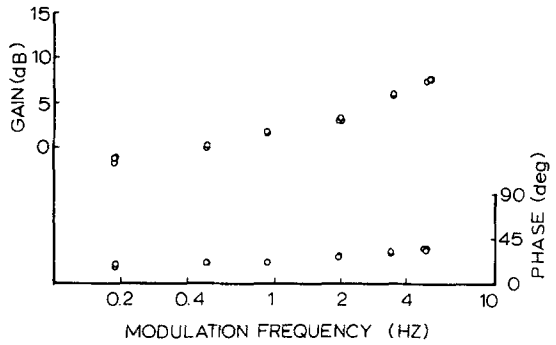

FIGURE 1. Stationarity and data reproducibility. Gain and phase data obtained from a slowly adapting stretch receptor of crayfish (tabulated in Table I) for three separate runs spaced 30 min apart are plotted as a function of modulation frequency. f_0 = 12 imp/s.

TABLE I
ANALYSIS OF DATA FROM THREE SEPARATE RUNS IN CRAYFISH RECEPTOR

Mod freq	Gain	Phase (deg)	Dist
Hz	*dB*	*degrees*	%
1.93	3.98	23.3	9.22
1.96	3.38	23.5	10.28
1.94	3.09	24.5	10.34
0.92	1.64	18.5	6.28
0.91	1.83	20.7	5.36
0.48	−0.03	15.2	6.67
0.48	−0.12	16.2	7.92
0.48	0.24	16.9	9.82
0.18	−1.20	17.8	3.65
0.18	−1.03	16.8	9.20
0.18	−2.20	12.7	14.75
4.97	7.64	30.2	13.82
4.93	7.27	32.0	10.38
5.00	7.76	32.6	8.53
3.46	5.94	27.8	11.57
3.46	6.08	29.3	8.25

f_0 = 12 imp/s (200 pulses per analysis).

potential fluctuations which contributed to noise in the output pulse train (Dodge et al., 1968; Shapley, 1971). The repeatability of the data points indicated that they were accurate to within about 1 dB, which was less than the accuracy of the data obtained from the stretch receptor.

Steady-State Frequency vs. Current Curves

To obtain data on steady-state frequencies, at least 200 and usually 500 impulses were timed, with the start of the data collection period set to commence after the first 30 s of the sustained stimulus period had elapsed. Data was obtained in the form of interval histograms in which the mean interval and the standard deviation were computed.

Data Analysis

The data analysis was performed on-line by using an IBM 1800 Data Acquisition and Control System (IBM Corp., White Plains, N. Y.). The analysis technique is fully described in the first paper of this series (Fohlmeister et al., 1977) and in our earlier papers (Poppele and Chen, 1972; Fohlmeister et al., 1974). Most of the cells reported were subject to both single sinusoidal and double sinusoidal analyses. In the latter case, a sinusoid is applied at a frequency equal to the spontaneous rate of the cell, f_0, and a second, smaller sinusoid is superimposed at various frequencies, ω. This procedure allows the determination of an equivalent γ designated γ_e (see Poppele and Chen, 1972; Fohlmeister et al., 1974) which is interpreted as that value of γ which the leaky integrator must have to give the same interspike interval ($1/f_0$) for the same stimulus conditions. Values determined from this analysis are tabulated in Tables II and III where they are expressed as γ_e/f_0, a ratio which has been found to remain nearly constant for a given cell.

In working with neuronal data, as opposed to model calculations or analog simulations, the interspike interval can only be defined statistically since there is a slight, random dispersion of interval length. In the crayfish receptor, the coefficient of variation of intervals is typically between 1.5% and 5%, and in the *Limulus* eccentric cell, about twice that large. Such variations are mostly accounted for by the averaging procedures used unless the variations become too large or the spike train is interrupted by double spiking (Hartline and Calvin, 1975) or by dropped spikes.

The distortion factor described in the previous paper (Fohlmeister et al., 1977) was used as a measure of the quality of the data analyzed. As previously discussed, factors other than "noise" contribute to this indicator, but if the noise is random and of modest intensity, then we should expect distortions calculated from neuronal data to approach those obtained with model data for the same depths of modulation.

For the crayfish stretch receptor, distortions were generally between 2% and 10% when the stated accuracy of 0.5 dB was achieved. For the eccentric cells, a distortion between 6% and 15% was usually obtained. Fig. 2 illustrates the fit of a sinusoid to binned data points in the presence of 6% (Fig. 2 A) and 4% (Fig. 2 B) harmonic distortion. Table I, which is a tabulation of the data presented in the Bode plot of Fig. 1, shows that the stated reproducibility level for crayfish could be obtained even when distortions approached 15%.

Models and Curve fitting

All experimental data which satisfied the criteria for stability stated above were subjected to a variation of parameters curve fitting to the leaky integrator model (see Fohlmeister et al., 1977). The results of this analysis are tabulated in Table II for the crayfish data and Table III for the *Limulus* data. In addition, several selected sets of data were fit to the variable-γ model. In these cases, model parameters ($\gamma[0]$, B and D) were selected to give the appropriate $\bar{\gamma}$ as calculated from the leaky integrator determinations. Feedback parameters (h/s_1 and τ) were the same as those found to provide the best fit for the leaky integrator.[1] Times of occurrence of impulses were then determined by numerical inte-

[1] As will be shown later in the paper the empirical quantity h/s_1, rather than h, provides the best quantitative estimate of summed feedback for the neuronal encoder.

gration and the resulting data set was analyzed with the same method used for the experimental data (for further details see Fohlmeister et al., 1974, 1977).

RESULTS

Slowly Adapting Stretch Receptor of Crayfish

Single receptor cells were impaled and depolarized with current to produce steady trains of action potentials at various frequencies f_0. Small sinusoidal modulations of this current at various frequencies ω resulted in modulated repetitive firing and resulting data are shown as Bode plots (see Fohlmeister et al., 1977, and Materials and Methods). As we reported in a previous paper (Fohlmeister et al., 1974), there is a systematic depression in gain for low

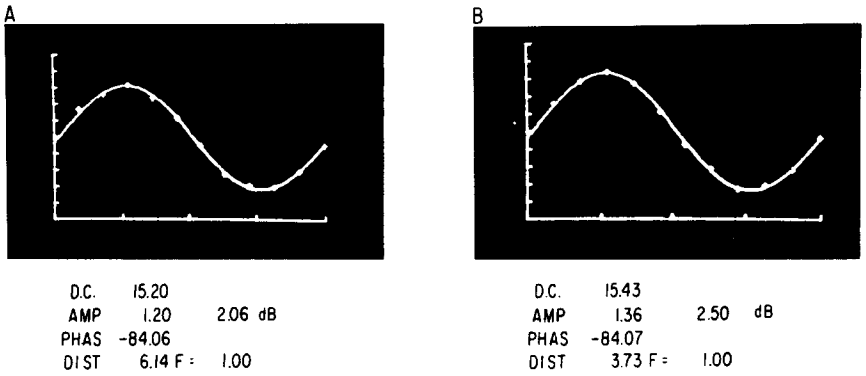

FIGURE 2. Interval analysis of crayfish receptor data. Points are reciprocals of average intervals computed for each of 11 bins (see Materials and Methods in Fohlmeister et al., 1977). Curve is drawn from the fundamental terms of the Fourier series that best fits the data points. A, Distortion is 6.14%. B, Data obtained from same unit at a different time; distortion is 3.73%. Amplitudes are within 0.52 dB and phases are the same. (The phase is given as $-84°$ instead of $+6°$ because the sync pulse of the stimulus generator occurred at the negative peak of the sinusoidal drive.)

modulation frequencies which cannot be accounted for by either the leaky-integrator or by the variable-γ model alone (note Figs. 2 and 3 in Fohlmeister et al., 1974).

This observation is illustrated again in Fig. 3. Data are plotted for nine receptors which were driven at $f_0 \cong 10$ imp/s. The solid line results from using a $\gamma = 30\ s^{-1}$ for the leaky integrator model (Eq. (I. 20), Fohlmeister et al., 1977). It can be seen that this curve fits all the data points whose modulation frequencies are above 3 Hz. Indeed, the value, $\gamma = 30\ s^{-1}$ was determined by using a variation of parameters analysis (Fohlmeister et al., 1977) which gave the best least mean square correspondence between the data points above 3 Hz and the gain equation for the leaky integrator. On the other hand, the behavior of the gain at frequencies below 3 Hz was such that if they were also included in the curve-fitting analysis, no value of γ for the leaky integrator could be found which provided an adequate fit.

The deviations from leaky integrator gain behavior in the low frequencies are similar to the effects of summed feedback on both the leaky-integrator and variable-γ models described in the companion paper (Fohlmeister et al., 1977). As seen in Fig. 3, the discrepancy between data and model was often small, though always systematic. Differences of the order of only 1 or 2 dB were not unusual, representing factors of 12%–25% in amplitude. Since data were generally reproducible to within 0.5 dB (or ±6% in amplitude), these differences were judged significant. Furthermore, we did observe larger effects (up to 8 dB or 250%) and we were able systematically to alter the effect by using procedures that are known to alter the behavior of an Na-K^+ ionic pump.

Fig. 4 shows the effect of removing external K^+. Bode data are plotted showing the response first in normal van Harreveld's soluton (vH), then in K^+-

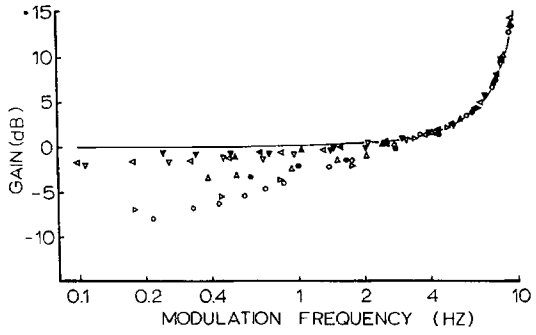

FIGURE 3. Gain data from crayfish receptor compared to leaky integrator model. Different symbols represent data from nine different receptors (identified in Table II) in which the dynamic behavior systematically deviates from the leaky integrator model gain that best fits the gain resonance beyond 3 Hz modulation. All gain values are normalized to 1 dB at 3.5 Hz. Leaky integrator parameters were $\gamma/f_0 = 3$ and $f_0 = 10$ imp/s with the same normalization.

free vH, and finally after 20 min of recovery in normal vH. Although the K^+-free perfusion produced a marked lowering of the cell resistance (from 9 MΩ to 3 MΩ) its behavior was stable and reproducible data could be obtained. Furthermore, the resistance recovered to 6 MΩ when it was again perfused with normal vH. Consider first the K^+-free data (open circles); the gain and low frequency phase were precisely fit by the leaky-integrator model with no feedback (solid curves). In generating the model curves, a threshold of 5 mV was used and the best fit was obtained with $\gamma/f_0 = 3.7$ $s_1/s_0 = 0.014$. The data obtained in normal vH (filled circles and triangles) could not be fit by the leaky-integrator model alone and it can be seen by inspection that the gain data are different. For these data the gain and low frequency phase could be reproduced by the leaky integrator with summed feedback. Again a 5-mV threshold was used and $\gamma/f_0 = 3.7$ still gave the best fit for the high frequency gain. For the data obtained before subjecting the cell to K^+-free vH, values of $s_1/s_0 = 0.02$, $h/s_1 = 1.2$, and $\tau = 0.1$ s provided the best fit. After recovery from the K^+-free vH in normal Ringers, the model indicates the h/s_1 was restored to 0.7 (58%) with the same τ of

0.1 s and s_1/s_0 became 0.022. Less complete data from two other cells treated with K^+-free vH showed the same changes as illustrated in Fig. 4. We were less successful, however, in abolishing the feedback with the cardiac glycoside, ouabain. For concentrations of 10^{-6} M there was no observable effect on the gain or phase. At 5×10^{-5} there was a detectable difference in gain with respect to normal which corresponded to a reduction in h to about 40% of its value in normal vH. At 4×10^{-4} M the difference was greater and corresponded to a reduction of about 60% of normal (see Table II, cells 17 and 18). This is the highest concentration we succeeded in producing without having the ouabain form a precipitate. Fig. 5 illustrates the gain and phase data for the case in which 4×10^{-4} M ouabain was used. Again the solid data points were obtained in

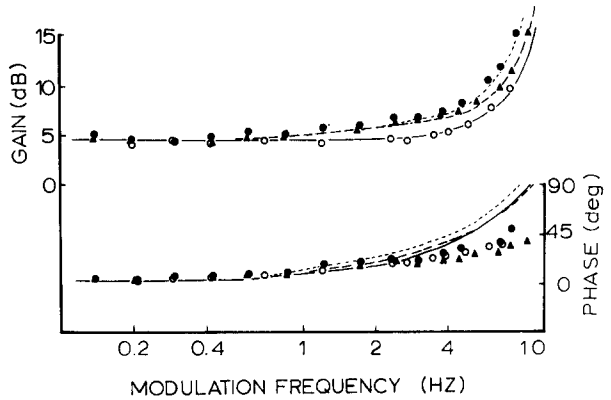

FIGURE 4. Effect of zero-K^+ on gain and phase. Symbols represent data obtained in normal Van Harreveld's solution (●), in K^+-free (○) and after returning to normal solution (▲). The dotted lines are plots of solutions to the leaky-integrator model equations with summed feedback which give the best least squares fit to the gain data in normal solution before K^+-free. Model parameters are tabulated in Table II, cell 4. The solid lines are plots of the leaky integrator model without summed feedback which fit gain data obtained in K-free. Dashed lines are model fits to data obtained after the cell was returned to normal solution.

normal vH and the leaky-integrator model fit indicates an $h/s_1 = 3.6$ and $\tau = 0.1$ s. After the cell was perfused with ouabain vH the open data points were obtained and they are compared to the leaky integrator without this feedback. The deviations from flat gain and zero phase at the lowest frequencies of modulation observed for this cell are described below.

If the feedback effects described above are induced by an electrogenic Na^+ pump, they would also be expected to be altered by lowering the temperature. This would increase the duration of the action potential and thereby allow more Na^+ to enter the cell per spike. It also would be expected to reduce the rate constant of the pump itself (Sokolove and Cooke, 1971). Normally, bath temperature was maintained at 15°C and we observed that most of the data obtained were consistent with a τ of 100 ms (except for two cells which had very large feedback: see Table II, cells 3 and 21). When the temperature was decreased to

10°C, τ increased to 150 ms and at 5° C it was 200 ms (Table II, cells 16 and 20). The data which illustrate the change that occurs when the temperature is reduced from 15°C to 5°C are plotted in Fig. 6. Not only was τ increased but h was also more than doubled, suggesting that the electrogenic pump is responding to the increased Na^+ loading that results from the increased spike duration. Notice also in Fig. 6 that the phase at 5°C is closely fit at all frequencies by the leaky-integrator model but not at 15°C. We will consider this point further in the discussion.

The three sets of data presented, the effect of K^+-free vH, the effect of ouabain, and the effect of temperature are all consistent with the hypothesis that the feedback mechanism responsible for the observed gain and phase is a metabolic ion pump that responds to intracellular Na^+ and requires extracellular K^+. Thus, there is qualitative agreement between our results and those of Nakajima and Takahashi (1966) and of Sokolove and Cooke (1971) who concluded that the post-tetanic hyperpolarization and adaptation of firing rate to step currents were due to an electrogenic Na^+ pump. However, the time constant described by the latter investigators was about 100-fold longer (i.e. about 10 s vs. the 0.1 s calculated from our data). Therefore, while the results described above are compatible with an electrogenic Na^+ pump, it may be a pump different from that responsible for the observed post-tetanic hyperpolarization in these receptors. As we will see below, a much longer time constant effect, which is quantitatively similar to that described in the earlier work, can also be identified by using sinusoidal current modulation.

The magnitude of the feedback effect we have described varied considerably among receptor cells, suggesting variations in the magnitude of electrogenic pumping (i.e., the extruded Na^+ not balanced by incoming K^+). In fact we found a correlation between the season of the year and the magnitude such that it was greatest in winter and smallest in summer (see Table II and Fig. 7). Many data obtained from receptors in summer months showed a negligible contribution by this particular feedback as illustrated in Fig. 7 A (open symbols) and also in Fig. 9. However, they did show evidence of a second summed feedback with a much longer time constant.

The second feedback affects the low-frequency (below 0.7 Hz) behavior of the receptor encoder. The low-frequency gain and phase data of cells showing the effect could be simulated by the leaky integrator model using $\tau = 3$ s and $h/s_1 = 0.2$ (so that $h \cdot \tau$ is approximately the same as the mean value for the short time constant feedback). As it was noted earlier, the low-frequency phase is particularly sensitive to feedback since the phase is near zero in the absence of feedback. Fig. 8 A is a composite plot from 10 cells of phase data in the range of 0.1–1.0 Hz. The shaded area represents the maximum phase advance due to the short time constant feedback alone. Data points are consistently above this level for frequencies below 0.3 Hz. The solid curve drawn through those points is for $\tau = 3$ s and $h/s_1 = 0.24$.

All the data points plotted in Fig. 8 A are from *C. astacus* and they represent all seasons of the year (see Table II). In most of the few experiments we did on *P. clarki* we did not observe the behavior to frequencies below 0.4 Hz, and above

TABLE II

EVALUATION OF FEEDBACK PARAMETERS IN CRAYFISH STRETCH RECEPTORS FROM SINUSOIDAL ANALYSIS

Cell	Date	f_0	$\frac{\tilde{\gamma}}{f_0}$	$\frac{\gamma_e}{f_0}$	$\frac{\tilde{\gamma}}{\gamma_e}$	$\frac{h_1}{s_1}$	t_1*	$\frac{h_1\tau_1}{f_0}$‡	$\frac{h_2}{s_1}$	τ_2*	Fig.	Species	Comment
1	1/13	9.0	2.5	–	–	2.3	0.10	25	0.03	15	9 B	Pc	
2	1/15	10.6	3.0	–	–	2.2	0.10	21	–	>8	3	Pc	
3	1/29	10.0	3.3	–	–	7.0	0.12	84	–	–	3	Ca	
4	2/28	9.0	3.7	–	–	1.2	0.10	12	–	>8	4	Pc	
	2/28	10.0	3.7	–	–	0	0	0	–	>8	4	Pc	K-free
5	3/7	7.4	4.0	1.6	2.5	2.0	0.10	27	–	>8		Pc	
6	3/15	13.6	3.2	0.7	4.5	2.5	0.10	19	–	–		Pc	
	3/15	19.8	2.5	0.5	5.0	3.7	0.10	19	–	–		Pc	
7	4/8	20.1	2.5	–	–	4.4	0.10	22	0.24	3	8 A	Ca	
8	8/15	8.5	3.2	–	–	1.0	0.10	12	–	–		Ca	
9	8/30	7.2	3.2	1.1	2.9	0.5	0.10	7	0.23	3	7 A, 9	Ca	
	8/30	14.1	2.8	–	–	1.2	0.10	9	0.23	3	9, 8 A	Ca	
10	9/2	14.4	3.0	0.7	4.3	1.2	0.10	8	0.23	3	9, 8 A	Ca	
	9/2	19.1	2.7	0.6	4.5	1.8	0.10	9	0.23	3	9, 8 A	Ca	
	9/2	31.5	2.9	0.5	5.8	2.5	0.10	8	0.23	3	8 A	Ca	
11	9/28	13.5	3.0	1.0	3.0	2.6	0.10	19	0.24	3	8 A	Ca	
12	10/6	20.5	2.5	1.0	2.5	4.7	0.10	24	–	–		Ca	
13	10/8	9.2	3.2	1.4	2.3	3.0	0.10	33	–	–	3	Ca	
	10/8	20.5	2.5	1.0	2.5	4.7	0.10	24	–	–		Ca	
14	10/13	9.0	3.2	1.9	1.7	2.2	0.10	24	–	–	3	Ca	
	10/13	18.5	3.0	1.2	2.5	4.5	0.10	24	–	–		Ca	
15	10/15	17.5	3.0	1.3	2.3	3.7	0.10	21	–	–		Ca	
16	10/23	7.5	3.5	–	–	2.9	0.10	40	–	>8	6	Pc	15°C
	10/23	7.0	3.5	–	–	6.3	0.20	180	–	>8	6	Pc	5°C

17	11/3	13.9	3.3	1.2	2.8	3.8	0.10	27	0.24	3	9 A	Ca	
	11/3	13.8	3.3	1.3	2.5	2.2	0.10	16	0.23	3	9 A	Ca	5×10^{-5} ouabain
18	11/12	10.4	3.5	1.2	2.9	3.6	0.10	35	0.23	3	3, 9 A	Ca	
	11/12	10.3	3.5	1.3	2.7	1.4	0.10	14	0.20	3	3, 9 A	Ca	4×10^{-4} ouabain
	11/12	20.0	3.0	0.8	3.8	7.9	0.10	40	0.24	3	9 A	Ca	
19	11/17	10.2	3.2	0.7	4.6	6.5	0.10	63	–	–	3, 9 A	Ca	
	11/17	19.8	3.5	0.7	5.0	7.9	0.10	40	–	–	9 A	Ca	10^{-5} ouabain
	11/17	18.9	3.0	0.8	3.8	10.0	0.10	53	–	–	3	Ca	
20	11/23	10.0	3.0	1.5	2.0	5.4	0.10	54	–	–	3	Ca	15°C
	11/23	10.1	3.0	1.4	2.1	5.4	0.15	108				Ca	10°C
21	12/1	6.0	3.2	1.4	2.3	5.7	0.20	186	0.15	3	7 A	Ca	
	12/1	11.9	3.2	1.3	2.5	6.0	0.20	100	0.15	3	3	Ca	
	12/1	20.2	3.0	1.2	2.5	6.0	0.20	59	–	–		Ca	
	Means		3.1±0.3	1.1	2.8	4.4	0.11	39	0.22	3		Ca	15 cells
			3.3±0.5	0.9	3.5	2.4	0.10	24	–	>8		Pc	6 cells

* Units are seconds.

‡ Units are normalized to 10^{-3} V·s/imp.

§ Pc = *Procambarus clarki*; Ca = *Cambarus astacus*.

that frequency we did not observe the effect of a long time constant feedback (e.g., Table II, cells 1, 2, 4, 5, 6, 16). However, in one cell which we stimulated at frequencies down to 0.01 Hz (Table II, cell 1) we found low-frequency phase leads compatible with a τ of 15 s (Fig. 8 B). For the others we could only

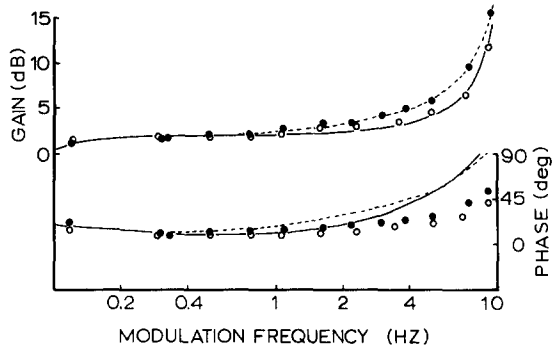

FIGURE 5. Effect of ouabain on gain and phase. Symbols represent data obtained in normal Van Harreveld's solution (●) and in 4×10^{-4} ouabain (○). The dotted lines are plots of solutions to the leaky integrator model equations with two summed feedbacks which give the best least squares fit to the gain and low frequency phase data in normal solution. Model parameters are given in Table II, cell 18. Solid lines are plots of leaky-integrator model with only the long time constant summed feedback (see text). f_0 = 10.3 imp/s without ouabain; f_0 = 10.4 imp/s with ouabain.

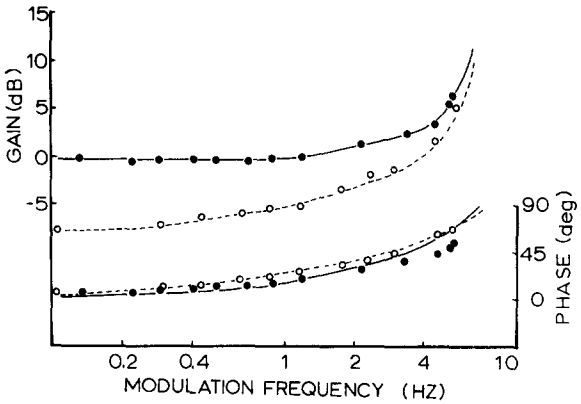

FIGURE 6. Effect of temperature on gain and phase. Symbols represent data obtained at 15°C (●) and 5°C (○) in the same crayfish receptor with f_0 = 7.5 imp/s. The curves are plots of solutions to the leaky integrator model equations with summed feedback which gave the best least squares fit to the gain data. Model parameters are given in Table II, cell 16. Note that at 5°C, the data fit both gain and phase of the leaky integrator.

determine that if there was a feedback of long time constant, that time constant must be greater than 8 s.

In Fig. 9 we have plotted complete sets of data from two cells that showed very little effect due to the short time constant feedback but did show the 3 s time con-

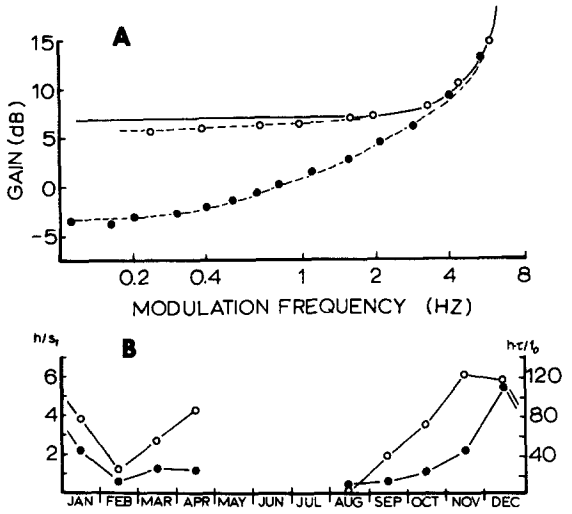

FIGURE 7. Seasonal variation of summed feedback in the crayfish receptor. A, Gain plots illustrating the extremes observed for the effects of summed feedback with short time constant. Minimum deviation from the leaky integrator gain was observed in late summer (O, cell 9 in Table II) and maximum in winter (●, cell 21 in Table II). B, Left ordinate and open symbols, mean values of h/s_1 for each month in which data were available. Right ordinate and solid symbols, mean values of the quantity $h \cdot \tau/f_0$ as tabulated in Table II.

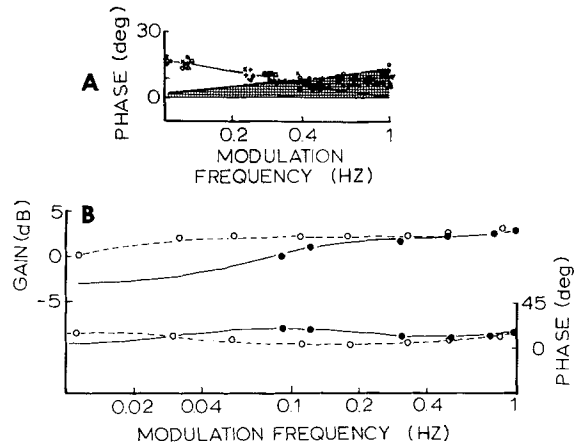

FIGURE 8. Long time-constant summed feedback in the crayfish receptor. A, Phase data from 10 *C. astacus* strech receptors obtained from August to April. Shaded area represents the maximum phase lead expected for the short time-constant feedback, corresponding to model parameters used for cell 21 in Table II. B, Comparison of low-frequency (0.01–1.0 Hz) behavior of *P. clarkii* (O) and *C. astacus* (●). Curves are plots of leaky-integrator model equations that provide the best least square fits to the respective data. Model parameters are given in Table II, cells 1 and 9.

stant effect clearly (Table II, cells 9 and 10). The leaky integrator model (solid line) required a $\gamma/f_0 = 3.0$ for $f_0 = 14.4$ Hz, and $\gamma/f_0 = 2.7$ for $f_0 = 19.1$ Hz with $s_1/s_0 = 0.017$ and 0.02, respectively. The low-frequency (below 1 Hz) gain and phase are well fit with the summed feedback parameters of $\tau = 3$ s and $h/s_1 = 0.23$.

The variable-γ model (open symbols) required a $B = 0.175$ ms^{-1}, $D = 10^{-5}$ ms^{-2} mV^{-1}, and a $\gamma(0) = 1.48$ ms^{-1}. With these parameter values we were able to get an exact high-frequency gain and phase fit at $f_0 = 14.4$. Since the model automatically satisfies the γ/f_0 = constant relationship (Fohlmeister et al., 1974), the same parameters led to the correct high frequency gain at $f_0 = 19.1$ Hz, but it did not reduce the high-frequency phase sufficiently to agree with the neuron data at $f_0 = 19.1$ Hz (solid triangles) for the same parameters B, D, and $\gamma(0)$. This point will be further amplified in the Discussion.

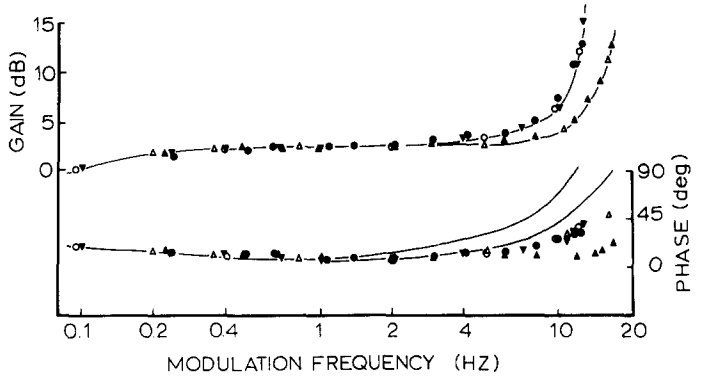

FIGURE 9. Comparison of stretch receptor data with leaky integrator and variable-γ models. Solid symbols are data from two crayfish stretch receptor cells at two values of f_0. Cells 8 (Table II, ●) and cell 9 (▼) data are plotted for $f_0 = 14.4$ imp/s and cell 9 (▲) again for $f_0 = 9.1$ imp/s. Solid lines are plots of leaky integrator model equations with summed feedback that best fit the gain data. Model parameters are given in Table II. Open symbols are gain and phase values obtained for the variable-γ model. In this case the model fits both gain and phase at $f_0 = 14.4$ imp/s but the phase at $f_0 = 19.1$ imp/s.

The gain and phase data for low frequencies (<0.7 Hz), which is the region pertinent to the 3-s summed feedback parameter analysis illustrated in Fig. 9, was fit well by $h/s_1 = 0.231$ (for the variable-γ model $h = 0.00547$ mV/ms, $s_1 = 0.0237$ mV/ms) and $\tau = 3$ s. Furthermore, for an assumed threshold of 9 mV the variable-γ model required an $s_0 = 0.409$ mV/ms for an f_0 of 14.4 Hz and an $s_0 = 0.569$ mV/ms for $f_0 = 19.1$ Hz. These values result in $s_1/s_0 = 0.0579$ at 14.4 Hz and $s_1/s_0 = 0.0417$ at 19.1 Hz, corresponding to ratios of current applied through the pipettes of $i_1/i_0 = 0.06$ at 14.4 imp/s and 0.04 at 19.1 imp/s. As we will argue in the Discussion, the close correspondence between the s_1/s_0 ratio of the model and the i_1/i_0 ratio (that is the ratio of modulating current to depolarizing current) is taken as evidence that the variable-γ model offers an accurate description of the total current loading seen by the electrode.

Both the 0.1-s and 3-s summed feedbacks described above should be expected to produce adaptation to a step of depolarizing current. The short τ is expected

to produce an initial rapid decay in firing rate whereas the second feedback effect should slowly decrease the firing rate for several seconds. Indeed, both effects have been observed. In Fig. 10 we have replotted published data obtained by other investigators (Jansen et al., 1971) along with semilog plots (Fig. 10 C) indicating the exponential nature of the frequency change. The crayfish data (recorded for 1.3 s after application of the current step) show a rapid decay in frequency with apparent time constant of about 60 ms and a slow decay with

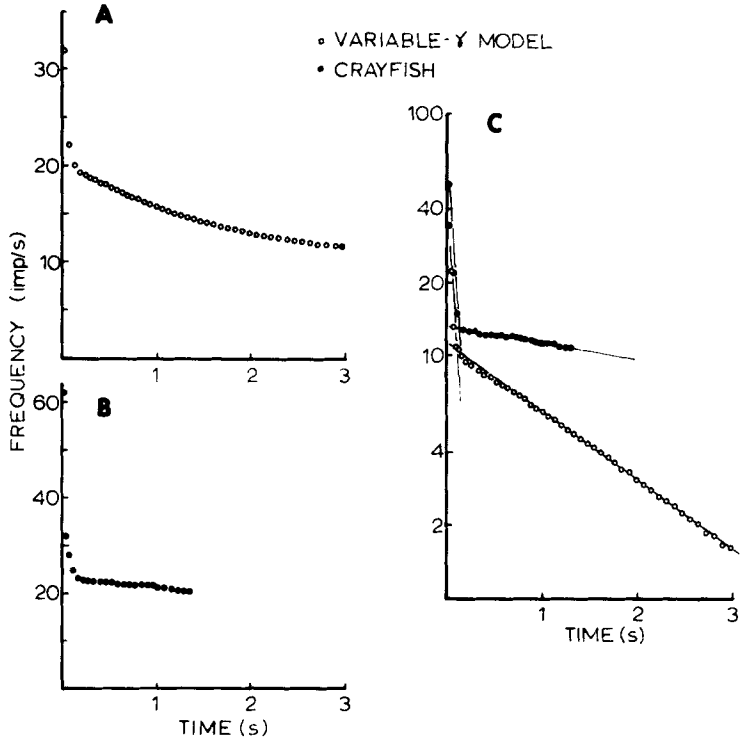

FIGURE 10. Response of crayfish receptor to current step compared to variable-γ model. A, Variable-γ model. Impulse frequency calculated as reciprocal intervals as a function of time after a step increase in s_0. Two summed feedbacks were included in the simulation, $\tau_1 = 0.1$ s and $\tau_2 = 3$ s. B, Response of stretch receptor from *A. fluviatus* to step of current applied intracellularly. Replotted from data presented by Jansen et al. (1971), Fig. 1. C, Semilog plots of points plotted in A and B.

apparent time constant of about 6.4 s. If the factor of 2.2 between τ_f and τ (Fohlmeister et al. 1977, Eq. [I.12]) proposed by Sokolove and Cooke (1971) is applicable to this receptor, then the data suggest that there are two summed feedback processes with actual time constants of 130 ms and 14 s, respectively.

In Fig. 10 A and open symbols in Fig. 10 C we plot the response of the variable-γ model (same γ parameters used for Fig. 9) to a step input. Two feedback terms were included, one with $\tau = 0.1$ s and $h = 0.164$ V/s, the other $\tau = 3$ s and h = 0.00547 V/s. The plots show that summed feedback does produce an exponential decay in frequency in this model. The early decay in frequency has a time

constant of 55 ms and the slow decay has a time constant of 1.65 s. For this model, the proportionality between the time constant of decay in frequency and τ is 1.8.

Previously we noted that the variable-γ model made certain predictions regarding the effect of a hyperpolarizing pulse applied to the cell after each spike in a repetitive train (Fohlmeister et al., 1974). In testing the predictions we have also observed that when the pulses were stopped abruptly the cell would often show a transient increase in its rate of firing, and we suspected that the hyperpolarizing pulses might also somehow interfere with the long time constant feedback mechanism. Indeed, by appropriately adjusting the parameters of the hyperpolarizing pulse we could completely abolish the low-frequency gain and phase changes induced by that feedback (Fig. 11). Therefore, whatever mecha-

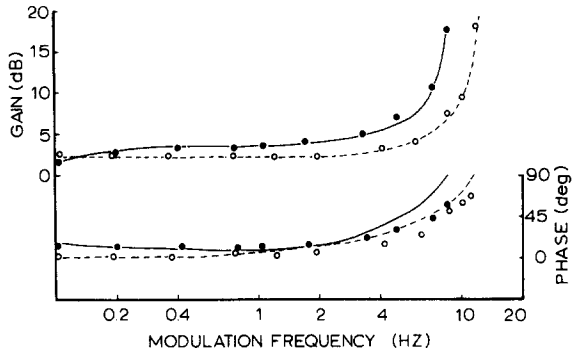

FIGURE 11. Effect of hyperpolarizing pulses on the long time constant summed feedback. Symbols represent data obtained under normal conditions (●) and with the application of a 2 nA hyperpolarizing pulse of 9 ms duration 2 ms after the peak of each action potential in the repetitive train (○). Solid lines are plots of leaky integrator model equations with summed feedback ($h/s_1 = 0.23, \tau = 3$ s, $f_0 = 10$ imp/s) and dashed lines without summed feedback ($f_0 = 12$ imp/s).

nism is responsible for this feedback effect, it seems to be influenced by the electric field across the membrane, or possibly the current through the membrane.

Finally, as shown in a companion paper (Fohlmeister et al., 1977), the steady-state frequency-current relationship is also affected by these feedback processes. In particular, by a judicious choice of k, τ_k, h, and τ, these steady-state curves can be made quite linear. However, the fact that many neurons are not only approximately linear in this regard but show in fact a proportionality between f_0 and s_0 requires the variable-γ model. Furthermore, for the crayfish receptor, the f_0 vs. i_0 curve is not exactly linear; the slope decreases for frequencies $f_0 > 20$ Hz (Terzuolo and Washizu, 1962). Fig. 12 (solid symbols) is a plot of f_0 vs. i_0 for two cells, one which showed only the short time constant feedback ($\tau = 0.1$ and $h/s_1 = 2.2$) and the other which showed only the 3-s feedback ($h/s_1 = 0.24$). The open symbols are plots of values obtained with the variable-γ model (same γ parameters as for Fig. 9). For the 0.1-s feedback (triangles), the proportionality factor C $= 4.22 \times 10^{-9}$ farads related the s_0 of the model to the i_0 injected into the cell,

since by definition, $i_0 = C \cdot s_0$. For the 3-s feedback (circles) the factor was 4.05×10^{-9} farads with an offset of 0.46 nA in the current axis.

Eccentric Cell of Limulus

Single sensory cells, identified as eccentric cells, were impaled and depolarized

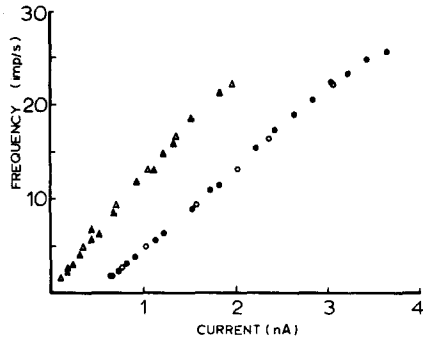

FIGURE 12. Steady state f_0 vs. i_0 curves for the crayfish receptor. Solid symbols are data obtained from two stretch receptors, one with no apparent long time constant feedback (▲) and the other with only a long time constant feedback, τ = 3 s (●). Open symbols were obtained from the variable-γ model.

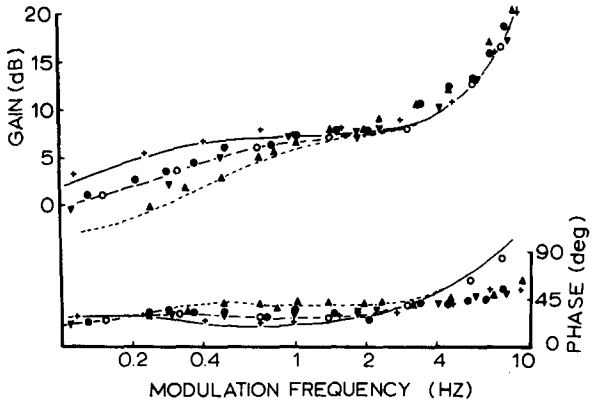

FIGURE 13. *Limulus* eccentric cell compared to leaky-integrator and variable-γ models with summed feedback. Solid symbols are data from four eccentric cells with $f_0 \doteq 10$ imp/s; +, ●, ▼, and ▲, cells 3, 4, 6, and 8 in Table III. Lines are plots of leaky integrator equations with a single summed feedback that give the best fit to gain and low frequency phase. Model parameters are given in Table III. Open symbols (○) are derived from the variable-γ model for one set of feedback parameters ($h/s_1 = 0.74$, $\tau = 1.0$).

with current to produce steady trains of action potentials. Small sinusoidal modulations of this current at various frequencies ω resulted in modulated repetitive firing. As before, the data are plotted as Bode plots (Figs. 13, 14, and 16).

Fig. 13 is a plot of data from four eccentric cells which illustrate the range of

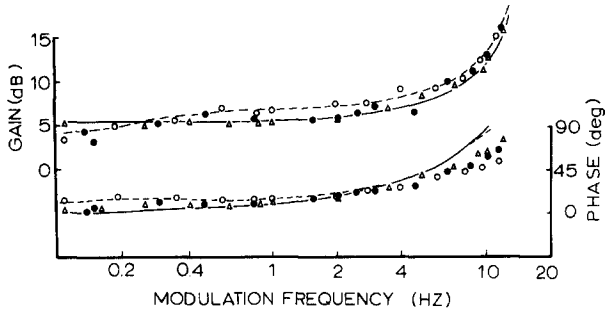

FIGURE 14. *Limulus* edge cell. Symbols represent data obtained from an eccentric cell on the edge of the *Limulus* lateral eye; (●) 10 mM K^+ (normal Ringer's), (○) 0.5 mM K^+, (△) 20 mM K^+. Solid lines are plots of leaky integrator equations with summed feedback ($h/s_1 = 2.3, \tau = 0.05$ s) that best fit the gain and low-frequency phase data obtained in normal Ringer's. Dashed lines are plots of equations with two summed feedbacks ($h_0/s_1 = 2.3, \gamma_1 = 0.05$ s; $h_2/s_1 = 0.22, \tau_2 = 1.0$ s). See Table III, cell 5.

TABLE III

EVALUATION OF FEEDBACK PARAMETERS IN *Limulus* ECCENTRIC CELL FROM SINUSOIDAL ANALYSIS

Cell	Date	f_0	$\frac{\bar{\gamma}}{f_0}$	$\frac{\gamma_e}{f_0}$	$\frac{\bar{\gamma}}{\gamma_e}$	$\frac{h}{s_1}$	τ*	$\frac{h \cdot \tau}{f_0}$‡	Fig.	Comment
1	8/16	11.0	6.0	2.0	3.0	0.93	0.7	59		
2	8/19	9.6	6.0	–	–	3.14	0.6	196		
3	8/20	9.2	6.5	1.3	5.0	1.56	0.8	126	13	
4	9/26	9.0	6.5	–	–	0.74	1.0	82	13	
	9/26	9.5	6.5	–	–	2.67	0.6	169		0.05 × K^+
	9/26	9.5	6.5	–	–	0.25	0.6	16		2 × K^+
5	11/20	15.0	6.7	–	–	0.10	1.0	7	14	edge cell
	11/20	15.0	6.7	–	–	0.20	1.0	14	14	0.05 × K^+
	11/20	15.0	6.7	–	–	0.0	–	0	14	2 × K^+
6	2/11	11.0	6.0	2.3	2.6	0.37	2.0	67	13	
	2/11	9.7	6.0	–	–	2.67	0.6	165		0.05 × K^+
	2/11	10.9	6.5	–	–	2.50	0.6	138		normal Ringer's
7	2/13	20.6	6.5	–	–	0.36	0.7	12		
8	2/18	10.4	6.5	–	–	0.74	1.0	71		
	2/18	15.0	7.0	–	–	0.60	0.8	32		2 × K^+
	2/18	8.6	6.5	–	–	0.90	1.0	105	13	Normal Ringer's
9	2/20	18.0	4.5	–	–	0.33	1.0	18	16	
	2/20	15.0	4.5	–	–	0.91	0.8	49	16	0.05 × K^+
	2/20	18.0	4.5	–	–	0.25	1.0	14	16	2 × K^+
	Means		6.1 ± .8	1.9	3.2	0.91	.97			

* Units are seconds.

‡ Units are 10^3 V.s/imp.

behavior seen in the cells investigated (see Table III). The solid points are plots of experimental data and the lines are plots of leaky-integrator simulations with threshold of 5 mV, $\gamma/f_0 = 6.5$, and $s_1/s_0 = 0.002$. It is clear from the data and verified by the simulation that these cells were subject to different magnitudes of feedback and that the time constants of that feedback were different. The latter

point is particularly evident in the phase data. The low-frequency maximum phase is around 0.6 Hz for $\tau = 0.8$ s and less than 0.2 Hz for $\tau = 2.0$ s. The range of values of feedback parameters determined in nine cells is tabulated in Table III.

The data plotted in Fig. 13 were all from cells for $f_0 = 10$ imp/s. In nine cells with f_0 ranging from 8.6 to 20.6 imp/s, we observed an average $\gamma/f_0 = 6.2$. This relationship was approximately independent of f_0 as was previously found for the crayfish receptor (Fohlmeister et al., 1974) and for the secondary muscle spindle receptor (Poppele and Chen, 1972). Furthermore, in three cells we also determined γ_e (see Materials and Methods) and found that the average γ_e/f_0 was 1.9. Thus, in the *Limulus* eccentric cell, the magnitude of γ is larger than that of the crayfish receptor, but the ratio $\gamma/\gamma_e = 3.2$ is approximately the same (cf. Table II for crayfish data). Compared with the crayfish receptor, data from eccentric cells required that the variable-γ model have a larger $\gamma(0)$ and a larger B in order for the model simulations to fit. This is consistent with the above observation that the magnitude of γ is larger in the eccentric cell. The open symbols in Fig. 13 show the variable-γ simulations with $\gamma(0) = 2.0$ ms^{-1}, $B = 0.045$ ms^{-1}, and $D = 10^{-5}$ mV^{-1} ms^{-2}. The h/s_1 and τ were the same as for the leaky integrator (dashed curve) but the $s_1/s_0 = 0.113$ which compares with the value of $i_1/i_0 = 0.1$ for these cells.

As illustrated in Fig. 13 the magnitude of self inhibition in these cells varies considerably. In Fig. 14 we have plotted data from a cell in which it was nearly absent (see also Table II, cell 5). This was an edge cell which is known to receive less lateral inhibition and also less self inhibition (Purple, unpublished observations) than more centrally located eccentric cells. The data in Fig. 14 (●) are compared with a leaky-integrator simulation (solid lines) with no long time constant feedback. However, we found that it was necessary to include a short time constant feedback ($\tau = 0.05$ s; $h/s_1 = 2.3$) since no solution to the leaky-integrator equations could be found to fit the high-frequency gain data without including a feedback term. This short time constant feedback is very similar to what was observed in the crayfish, but with a time constant only half as long. The effect is most easily observed in the edge cell, although the gain data of two cells plotted in Fig. 13 also show behavior between 2 Hz and 6 Hz that is likely to be due to the same effect. We did not explore further this finding, although it seems likely that it may also be due to electrogenic pumping of Na^+.

If self inhibition is a hyperpolarization induced by an increase in g_K (Purple, 1969), then changes in extracellular $[K^+]$ should alter the magnitude of that hyperpolarization. As shown in Fig. 15, the difference between the resting potential and the reversal potential for self inhibition does vary with external $[K^+]$. Its effect on the magnitude of inhibition as observed in the Bode data can be seen in Figs. 14 and 16. In Fig. 14 the lowering of $[K^+]$ from its normal value of 10 mM to 0.5 mM enhanced the small amount of inhibition present. Compare the open circles to the dashed line which is a leaky integrator simulation with a second summed feedback $h_2/s_1 = 0.22$ and $\tau_2 = 1.0$ s. The open triangles represent data obtained at 20 mM K^+ and they show an apparent absence of the long time constant effect.

Data from another cell (not an edge cell) illustrated in Fig. 16 show the same

general features, an increase in feedback magnitude at 0.5 mM K^+ and a decrease in that magnitude at 20 mM K^+. It was also found that low external [K] decreased the time constant of the feedback, in this case from 1.0 s to 0.8 s. This was a consistent observation in these cells as long as sufficient time was allowed for the change of solution to take effect (Purple, 1969).

As a final point, it is well known that the eccentric cell adapts to a constant

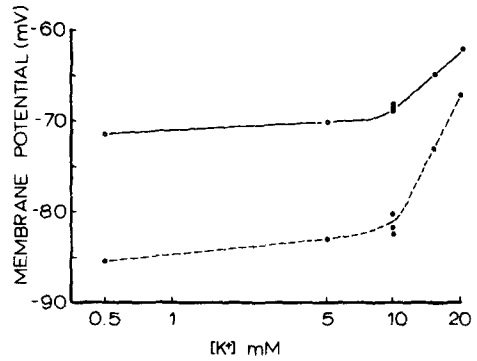

FIGURE 15. Effect of $[K^+]$ on resting membrane potential and on self inhibition in *Limulus*. Open symbols plot membrane resting potential and solid symbols plot the equilibrium potential for self inhibition.

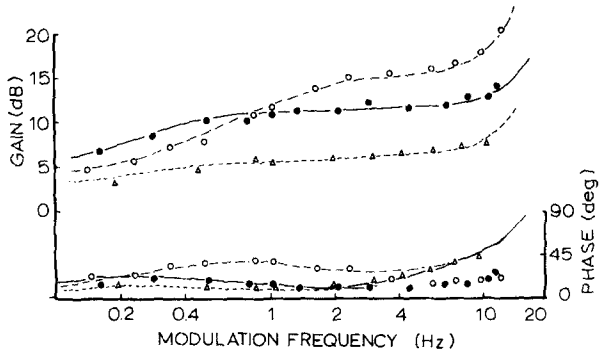

FIGURE 16. Effect of $[K^+]$ on gain and phase. Symbols represent data obtained from a *Limulus* eccentric cell in normal Ringer's, 10 mM K^+, (●), in 0.5 mM K^+ (○), and 20 mM K^+ (△). Curves are plots of leaky integrator model equations with summed feedback that best fit the gain and low-frequency phase data. Model parameters are given in Table III, cell 9.

current step (Fuortes and Montegazzine, 1962). In Fig. 17 we show that the feedback due to self inhibition can completely account for that adaptation. Fig. 17 A is a plot of data previously published by Stevens (1964) and Fig. 17 B is a plot obtained by simulation with the variable-γ model using the same parameters used for the simulation in Fig. 13.

DISCUSSION

The results of the experiments reported above and the analysis of those results lead to the following conclusions.

All of the observed encoder adaptation can be accounted for by spike-locked inhibitory summed feedback. No accommodative or nonspike-activated mechanisms are required, and if present, their effects are likely to be small. This is because the Bode data are taken in a quasi-steady state condition of a nearly constant current stimulation, and feedback parameters deduced from the analysis of that data account for all of the adaptation observed in the step response.

Both the slowly adapting stretch receptor of crayfish and the eccentric cell of *Limulus* appear to have at least two summed feedback mechanisms which affect encoder behavior in different regions of the frequency domain and therefore have different rate constants.

The effects of zero external $[K^+]$, oubain, and lowered temperature were consistent with the hypothesis that the short time constant feedback observed in the crayfish receptor is due to the electrogenic component of an Na^+-K^+ pump

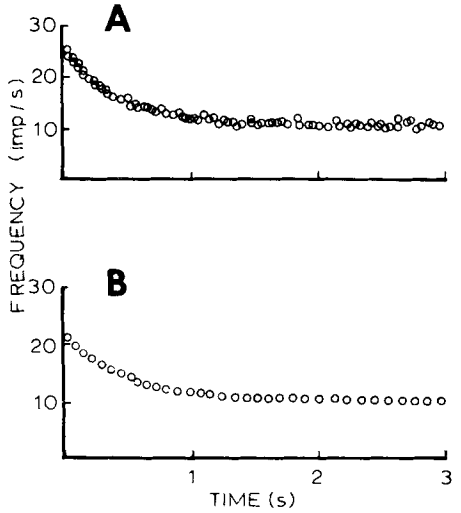

FIGURE 17. Response of *Limulus* eccentric cell to current step compared to variable-γ model. A, Composite of data obtained from *Limulus* eccentric cell previously published in Purple (1964). B, Response of variable-γ model to step change in s_0 with model parameters used in Fig. 13.

activated by the Na^+ entering the cell with each action potential. This appears to be a separate mechanism from that previously described (Nakajima and Takahashi, 1966; Sokolove and Cooke, 1971) because of the much more rapid rate constant. The observed seasonal dependence seems to reflect a seasonal variation in the magnitude of electrogenic pumping.

The long time constant feedback observed in the crayfish receptor is similar to that previously described by Nakajima and Takahashi (1966) and later quantitated by Sokolove and Cooke (1971). The latter authors reported the feedback primarily for *Orconectes virilis* and determined its time constant by two different techniques as 9.5 ± 2.9 s and 11.1 ± 3.4 s, respectively. These values are about threefold greater than the 3 s we report for *C. astacus* but similar to the value we found for *P. clarki*. Data from the Norwegian crayfish *Astacus fluviatilis*, plotted

in Fig. 10, suggest a long time constant of around 14 s which is quite close to our determination of 15 s for *P. clarki*. Although we did not specifically test the long time constant feedback to see if it was due to a Na^+ pump, we propose that it is the same mechanism as described previously and that its rate constant is more rapid in the Minnesota species. If so, then the new finding about this mechanism is the effect of hyperpolarizing pulses. The data presented in Fig. 11 strongly suggest that appropriate changes in the membrane electric field can abolish the electrogenic component of an Na^+ pump. This is further supported by our observation that when the hyperpolarizing pulses are turned off, after having been applied after each action potential in a long train, the rate of firing adapts as if a new current step had been applied. Therefore, feedback becomes suddenly active again when the hyperpolarizing pulses are stopped.

The eccentric cell of *Limulus* has a summed feedback which dominates its behavior to sinusoidally modulated current and is due to self inhibition (see also Knight, 1972; Dodge et al., 1968). The effects of varying external $[K^+]$ are consistent with the hypothesis that the feedback is primarily due to a potassium current (Purple, 1969; Purple, unpublished observations). The magnitude and time constant varied considerably among the cells studied and this presumably reflects the extent of self inhibition in these cells and their cable geometry. (There was some tendency for short time constants to be associated with larger magnitudes, see Table III.)

The interpretations and conclusions stated above mostly depend on the validity of the basic assumption made in the data analysis; that is, the feedback affects the encoder by reducing the effective drive. It should be noted that feedback which acts on membrane conductance will lead to similar experimental results, however, a quantitation of its magnitude cannot be made accurately because the equations cannot be solved in closed form.[2] In either case, the inclusion of a time-varying load, $\gamma(t)$, in the interspike interval does not affect the interpretations or the quantitation of the feedback parameters.

In the case of the Na^+ pump, it is reasonable that the basic assumption is correct. As shown by Nakajima and Takahashi (1966) there are no conductance changes associated with the hyperpolarization generated by the pump. Furthermore, the electrogenic component of current is directly across the membrane with little longitudinal component in the membrane where the spike is propagated (cf. Fig. 18). The case of self inhibition is different, however. Conductance changes in the eccentric cell soma have been measured that are presumably due to this mechanism (Purple and Dodge, 1965). Therefore conductance changes might well contribute to the observed gain and phase. The changes in gain and phase observed with alterations in external $[K^+]$ suggest, however, that they do not. Unless we postulate that the conductance change induced by the inhibitory synaptic transmitter is altered by $[K^+]$, then the same conductance change is expected in high and low external K^+. The gain and phase were altered in a way that is consistent with expected changes in potassium current as the potassium equilibrium potential is shifted closer to and further from the membrane resting potential. This still does not rule out the possibility that both conductance and

[2] J. F. Fohlmeister. Manuscript in preparation.

current changes may participate in determining the gain and phase but it strongly suggests that the responses to current feedback are dominant. We conclude, therefore, that in crayfish receptors, the feedback acts as an alteration of driving current and that in *Limulus* it is primarily the same, although some contribution by conductance changes may also be present.

To adequately describe repetitive firing, it is of primary importance to consider its normal operation rather than its operation in the context of a space-clamped membrane (Fohlmeister et al., 1974). This is evident from the facts that longitudinal current from the soma is responsible for trigger zone excitation and that soma depolarization is essential for high rates of repetitive firing (Nakajima

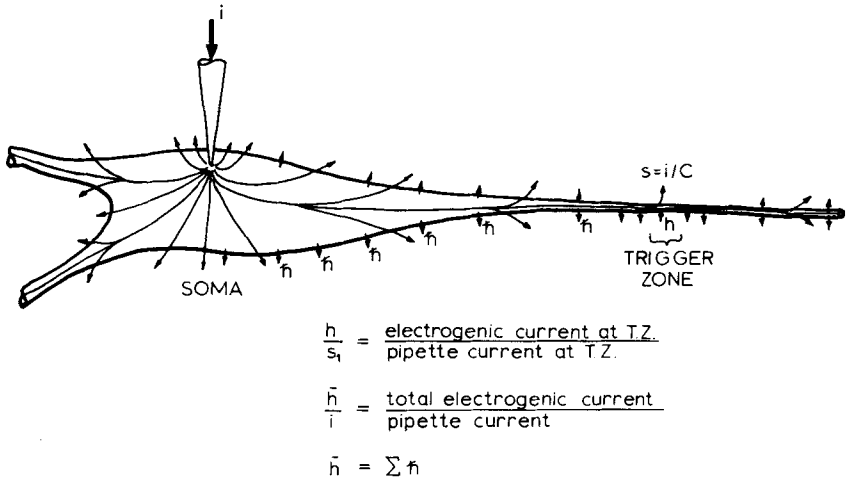

FIGURE 18. Current distribution in crayfish receptor. Schematic representation of how pipette current i is distributed to trigger zone. Drive at the trigger zone s is related to i by the factor C. Electrogenic current due to Na^+ pumping is assumed to be evenly distributed along the excitable membrane and its value at the trigger zone is h. See text for further explanation.

and Onodera, 1969). Therefore, because the encoder is not space clamped, the elements g and C entering the definition of γ in the equation:

$$\dot{u} = -\gamma \cdot u + s - H(t) \equiv -(g/C)u + i/C - H(t),$$

(see Fohlmeister et al., 1977) may not refer to specific transmembrane parameters. Here we do not attempt to interpret further the kinetics of g or C but restrict ourselves to a description of $\gamma(t)$ and $H(t)$. The Bode data are very sensitive to the functional dependence $\gamma(t)$ and $H(t)$ in different frequency regions of the gain and phase plots.

We noted in the results that h/s_1 as determined from the Bode analysis was equal for the leaky integrator and variable-γ models. This result, however, is true only if γ for the leaky integrator is first matched to the $\bar{\gamma}$ of the variable-γ model by superposing the gain resonance half-widths. This implies that the low frequency phase is sensitive to the "average" load $\bar{\gamma}$ in the presence of summed feedback, but not to details of the functional form of $\gamma(t)$.

Since we have focused on information contained in the train of action potentials generated at the trigger zone, that information must refer to that particular part of the cell; thus our data relate to events occurring at the trigger zone. The feedback magnitude h/s_1 represents a ratio of transmembrane currents at the site of spike initiation (see Fig. 18). If we assume that the current density at the trigger zone is about equal to the average current density over the entire excitable membrane,[3] then we can equate the h/s_1 ratio with $\bar{h}/i_1$, the ratio of the total electrogenic current to the pipette current. In that case, the total net charge becomes

$$\bar{h} \cdot \tau = h/s_1 \cdot \tau \cdot i_1.$$

For the typical value of i_1 used in most of our experiments, 0.2×10^{-9} A, we find that for each of the presumed Na^+ pumps described in the results for the crayfish receptor there is an average net charge of about 1×10^{-10} C pumped per spike (see values in Table II). The amount of Na^+ charge entering a cell per spike is approximately 8×10^{-7} C/cm^2 (cf. Palti, 1971). If we assume that the cell excitable membrane area is on the order of 5×10^{-4} cm^2,[4] then about 4×10^{-10} C of Na^+ charge enter the cell per spike. Thus it would appear that the electrogenic component for each sodium pump is four sodium ions pumped out for every three potassium ions pumped in. Although this number must be looked upon as only approximate because of the uncertainties about the assumptions made in arriving at it, it is remarkably close to the estimate arrived at by Nakajima and Takahashi (1966) based on an entirely different set of calculations and is therefore consistent with an interpretation of the Bode analysis results as indicating a summed feedback due to an electrogenic Na^+ pump.

In addition to the seasonal variation of the short time constant feedback, its magnitude was also observed to vary with f_0 in several cells. (See Table II, cells 6, 9, 10, 13, 14, and 19.) That variation was such that h/f_0 was approximately constant. The effect was not observed for the long time constant feedback (e.g., cell 9). It means that as the cell fires more rapidly, the total net charge pumped out per spike ($h \cdot \tau$) increases proportionally. The one cell in which this ratio did not remain constant (cell 21) was one in which h/s_1 was already very large, so it appears that there is a maximum above which the electrogenic component will not increase.

Whereas a determination of h from the Bode data leads to only approximate statements about the magnitude of electrogenic current due to the pumps, the existence of summed feedbacks and the values of their time constants may be accurately established. It is clear from the Bode data and confirmed by the transient response that two summed feedbacks, one with $\tau = 0.1$ s and the other

[3] Ringham (1971) has indicated that the trigger zone in the slowly adapting receptor is 270–340 μm from the cell soma. If we assume that the axon is a uniform cable with a diameter of 10 μm, with axoplasmic resistivity of 60 Ω-cm, and membrane resistance of 3,000 Ω/cm^2 (Katz, 1966), then this distance represents around 0.3 space constants from the cell soma. With these same assumptions, about 25% of the axonally directed current injected at the soma will leak out between the soma and the trigger zone. Therefore it is probably reasonable to assume that the trigger zone current density is nearly the average current density.

[4] Calculated for a typical slowly adapting receptor in crayfish as drawn in Florey and Florey (1955), if one assumes that the spike invades portions of the dendrites (Washizu and Terzuolo, 1966).

with τ = 3–15 s, are operating in the normal, slowly adapting stretch receptor of crayfish.

The data do not say very much about the locations of these membrane mechanisms, however. Both produce feedback locked to the rate of action potentials, so both must be within close enough proximity to the regenerative membrane to register effects of Na loading due to repetitive firing. Whether one may be located primarily in the soma-dendritic portion of the cell and the other in the axon or whether they are intermixed is one unanswered question raised by our findings. A second such question is that of the utility of two electrogenic pumps differing at least in their time constants. While their different effects on gain and phase responses to cyclical inputs and their different effects on relaxation rates to step inputs are clear enough, it is also possible that the different time constants could reflect a selective advantage geared to the need to cope with differential Na loading in various portions of the cell.

While the conclusions on both the existence of and time constants for the two summed feedbacks are in a sense model independent, the relation of a model's s_1/s_0 ratio to the i_1/i_0 ratio used experimentally is strongly model dependent. Therefore, it is significant that the variable-γ model simulations gave ratios $s_1/s_0 \doteq i_1/i_0$. Since both i_1 and i_0 are injected by the same electrode, their relative effects at the trigger zone must be in the same proportion as their magnitudes at the electrode. Any proportionality constant between i and s may, for present purposes be absorbed in the factor C. This factor, with units of capacitance, therefore becomes a measure of current distribution within the cell (Fig. 18). Its value can be estimated in the context of the variable-γ model from the relationship $s = i/C$. In fact, the steady-state data and the Bode data from the crayfish receptor provide for independent determinations of C. From the steady-state curves, we found that $C = 4 \times 10^{-9}$ F was the ratio of i_0/s_0 that was required to give a superposition of the variable-γ model and neuron curves. For the Bode simulation in another neuron (Fig. 9) we found that $s_1 = 0.0237$ mV/ms was required to match the gain level of the neuronal data obtained with $i_1 = 0.12 \times 10^{-9}$ A. This gives a ratio $i_1/s_1 = C = 5 \times 10^{-9}$ F. Furthermore, the i_1/i_0 ratios used in obtaining the Bode data were in close agreement with the variable-γ model s_1/s_0 ratios. Therefore, we suggest that the s_1 required in the variable-γ model is also the appropriate value for the cell in order to match the gain load of the model to that of the cell.

It is also significant that the determination of "total capacity" in the context of this model agrees with values that have been determined by more direct means. Nakajima and Onodera (1969) found a range of 3–4.8 $\times 10^{-9}$ F in 15 cells and Washizu and Terzuolo (1962) found an average cell resistance of 3.1 MΩ and average time constant of 14 ms, giving an average capacity of 4.5×10^{-9} F. Thus agreement between parameter determinations made with the variable-γ model and the direct measurements of those parameters constitute evidence for a basic level of validity of the function $\gamma(t)$ in the variable-γ model.

In contrast if we examine the values for the leaky integrator model, we find that s_1/s_0 is very much smaller for the same data. This very small ratio results for two reasons: (*a*) the γ of the leaky integrator is considerably larger than the $\gamma(t)$ of the variable-γ model in the mid and late parts of the interspike interval (see

Fohlmeister et al., 1974, Fig. 6), thereby requiring a larger s_0 to bring the voltage to threshold; and (*b*) because of this late loading the potential trajectory intercepts threshold at a shallow angle leading to a greater pulse frequency modulation for a given s_1. Thus it is clear that γ must be very small, at least late in the interval, in order that the s_1/s_0 ratio be correct; at the same time a mean value of γ, $\bar{\gamma}$, over the interval is determined by the resonance half-width of the gain curve (Fohlmeister et al., 1974).

During repetitive firing of a neuron, a resting potential does not exist, therefore the definition of a value for threshold level must be clarified. The threshold value of 9 mV used for the simulations with the variable-γ model is relative to the zero of the membrane potential variable u. (If depolarizing membrane current is assumed to be all K^+ current, then $u = 0$ is the potassium reversal potential E_K; cf. Nakajima and Takashi, 1966). This generally means that a 9-mV threshold corresponds to 8–8.5 mV above the lowest point of the postspike undershoot (See Eyzaguirre and Kuffler, 1955, Fig. 6 D). We find, however, that simulations with the variable-γ model are not sensitive to threshold level. In fact, if threshold is increased to 30 mV, the s_1/s_0 ratio changes by less than 4%.

Without becoming involved with detailed dynamics or mechanisms responsible for the particular function $\gamma(t)$,[2] we do need to make some comments on the parameters of the variable-γ model required for a simulation of encoder function. There are three parameters ($\gamma[0]$, B, D) which may be adjusted for simulations. As stated elsewhere, the proper loading requires a large γ early in the interspike interval and a small γ in the late portion of the interval. The initial value, $\gamma(0)$, is therefore a measure of the magnitude of the large portion of $\gamma(t)$. The parameter D determines how small γ will be in the late portion, and B controls how fast γ falls to the small value. A small B will cause $\bar{\gamma}$ enhancement as determined from resonance half-width. A large B will reduce the high-frequency phase. In order to achieve a simultaneous high frequency gain and phase fit with a single B, $\gamma(0)$ is adjusted to a particular (large) value. But, unless $\gamma(t)$ is very small in the late part of the interval, and unless B is sufficiently large so that $\gamma(t)$ reaches that small value early, the high-frequency phase has strong tendencies to revert to the (large) leaky integrator value; this despite the remaining sizable variations in $\gamma(t)$.[5] On the basis of this observation, we suggest that the high-frequency phase lead seen for the crayfish neuron when the data were taken at 5°C (Fig. 6) indicates that the low temperature slows down the kinetics of $\gamma(t)$—decreases B—as well as increases the time constant of the electrogenic pump.

In this connection we would point out that the high-frequency phase for the *Limulus* was not adequately reduced in the simulation (Fig. 13). This reduction would have required a certain very large $\gamma(0)$ which in turn would have necessitated a very short integration interval for the numerical integration of the variable-γ equations. We were limited, therefore, not by the model's ability to fit the data but by the prohibitive computer time that this would have entailed for the approximately 1,000 interspike intervals required for a complete Bode plot.

[5] This phenomenon is seen in our *Limulus*—simulation (Fig. 13) described earlier.

A further point that needs to be clarified in connection with the phase is the question of how great is the phase shift due to electrotonic lag between driving current at the electrode and the trigger zone. To determine this, we connected a lumped cable analog to a sine wave generator and measured the phase shift at various electrotonic distances from the source current. We further calculated that the trigger zone is about one-third of a space constant from the soma, and at this distance we found an electrotonic phase shift of 15° at f_m = 10 Hz and of 20° at f_m = 20 Hz. (This is consistent with direct measurements of current and voltage in crayfish receptors; Handelman and Purple, unpublished observations.) For smaller ω, the shift is relatively smaller. These estimates imply that the measured neuronal phase will be too small by amounts up to the above quoted values as compared with a phase measured with the electrode tip at the trigger zone. This phase depression at large ω is not of sufficient magnitude to account for the relative neuronal phase depression seen in going from f_0 = 14.4 Hz to 19.1 Hz for the data in Fig. 9. It can be seen in that data that the phase is clearly a function of f_0 and not just a function of ω. The explanation that is consistent with our findings on the phase sensitivity at these higher frequencies is that the large initial γ drops abruptly, leading to a long small-γ portion of the interval even at the higher frequency f_0. The present formulation of the variable-γ model does not accomplish this without using extremely large and unlikely values of $\gamma(0)$. Thus, although the variable-γ model shows the characteristics of neuron encoder dynamics, it still requires refinements to account for specific details. The Bode information suggests that $\gamma(t)$ may be more properly expressed by a second-order differential equation, or alternatively, as the product of two first-order variables. Even so, the variable-γ model does account quantitatively for all aspects of encoder behavior as well as for factors necessary for feedback. It therefore represents a sufficient model for repetitive firing in the sensory neurons investigated by us.

The specific mechanisms of summed feedback are quantitatively identified and their parameters can be directly related to model parameters. The basic mechanism of repetitive firing is accounted for by the state variable $\gamma(t)$ which has no known mechanistic correlate. If $\gamma(t)$ is shown to be conductance and capacitance as in $\gamma = g/C$, then we can determine from arguments presented above how the weighted mean of $\gamma(t)$, $\bar{\gamma}$ is distributed between these factors. An interspike interval of 100 ms and a $\bar{\gamma} = 30\ s^{-1}$ would suggest that the "mean" capacity is about 4.5×10^{-9} F and the "mean" cell conductance is about 1.35×10^{-7} mho. Since it is conceivable that both of the values vary in the interspike interval, we must now attempt to identify appropriate cellular mechanisms that can quantitatively account for these observations.

This work was supported by United States Public Health Service grants NS11695 and EY00293 and by National Science Foundation grant no. 76-10791. Computer facilities were made available by the United States Air Force Office of Scientific Research, grants nos. AFOSR-71-1969 and 75-2804.

Received for publication 27 July 1976.

REFERENCES

ADOLPH, A. R. 1976. Putative synaptic mechanism of inhibition in *Limulus* lateral eye. *J. Gen. Physiol.* **67**:417–432.

DODGE, F. A., B. W. KNIGHT, and J. TOYODA. 1968. Voltage noise in *Limulus* visual cells. *Science (Wash. D. C.)*. **160**:88.

DRILHON-COURTOIS, A. 1934. Minerals in crustacea. *Ann. Physiol.* **10**:377–414.

EDWARDS, C., C. A. TERZUOLO, and Y. WASHIZU. 1963. The effect of changes of the ionic environment upon an isolated crustacean sensory neuron. *J. Neurophysiol.* **26**:948–957.

EYZAGUIRRE, C., and S. W. KUFFLER. 1955. Processes of excitation in the dendrites and in the soma of single isolated sensory nerve cells of the lobster and crayfish. *J. Gen. Physiol.* **39**:87–119.

FLOREY, E., and E. FLOREY. 1955. Microanatomy of the abdominal stretch receptors of the crayfish (*Astacus fluviatilis* L.). *J. Gen. Physiol.* **39**:69–85.

FOHLMEISTER, J. 1973. A model for phasic and tonic repetitively firing neuronal encoders. *Kybernetik.* **13**:104–112.

FOHLMEISTER, J. F., R. E. POPPELE, and R. L. PURPLE. 1974. Repetitive firing: dynamic behavior of sensory neurons reconciled with a quantitative model. *J. Neurophysiol.* **37**:1213–1227.

FOHLMEISTER, J. F., R. E. POPPELE, and R. L. PURPLE. 1977. Repetitive firing: a quantitative study of feedback in model encoders. *J. Gen. Physiol.* **69**:815–848.

FUORTES, M. G. F., and F. MATEGAZZINI. 1962. Interpretation of the repetitive firing of nerve cells. *J. Gen. Physiol.* **45**:1163–1179.

HARTLINE, D. K., and W. H. CALVIN. 1975. Extra spikes in lobster stretch receptors: origin from spatial interaction and creation of metastable states. *Neurosci. Abstr.* **1**:592.

JANSEN, J. K. S., A. NJÅ, K. ORMSTAD, and L. WALLØE. 1971. Inhibitory control of the abdominal stretch receptors of the crayfish. III. The accessory reflex as a recruitment of inhibitory feedback. *Acta Physiol. Scand.* **81**:472–483.

KATZ, B. 1966. Nerve, Muscle and Synapse. McGraw-Hill Book Publishing Company, New York.

KNIGHT, B. W. 1972. The relationship between the firing rate of a single neuron and the level of activity of a population of neurons. *J. Gen. Physiol.* **59**:767–778.

NAKAJIMA, S., and K. ONODERA. 1969. Membrane properties of the stretch receptor neurones of crayfish with particular reference to mechanisms of sensory adaptation. *J. Physiol. (Lond.)*. **200**:161–185.

NAKAJIMA, S., and K. TAKAHASHI. 1966. Post-tetanic hyperpolarization and electrogenic Na pump in stretch receptor neurone of crayfish. *J. Physiol. (Lond.)*. **187**:105–127.

OBARA, S., and H. GRUNDFEST. 1968. Effects of lithium on different membrane components of crayfish stretch receptor neurons. *J. Gen. Physiol.* **51**:635–654.

PALTI, Y. 1972. Analysis and reconstruction of axon membrane action potential. *In* Biophysics and Physiology of Excitable Membranes. W. J. Adelman, Jr., editor. Van Nostrand Reinhold Co., New York. 206–284.

POPPELE, R. E., and W. J. CHEN. 1972. Repetitive firing behavior of mammalian muscle spindle. *J. Neurophysiol.* **35**:357–364.

PURPLE, R. L. 1964. Integration of excitatory and inhibitory influences in the eccentric cell in the eye of *Limulus*. Ph.D. Thesis. The Rockefeller University, New York.

PURPLE, R. L. 1969. Effects of ion substitution and altered calcium-magnesium ratios on lateral inhibition in *Limulus*. *Fed. Proc.* **28**:104.

PURPLE, R. L., and F. A. DODGE. 1965. Interaction of excitation and inhibition in the eccentric cell in the eye of *Limulus*. *Cold Spring Harbor Symp. Quant. Biol.* **30**:529–538.

RINGHAM, G. L. 1971. Origin of nerve impulse in slowly adapting stretch receptor of crayfish. *J. Neurophysiol.* **34**:773–784.

SHAPLEY, R. 1971. Fluctuations of the impulse rate in *Limulus* eccentric cells. *J. Gen. Physiol.* **57**:539–556.

SOKOLOVE, P. G., and J. M. COOKE. 1971. Inhibition of impulse activity in a sensory neuron by an electrogenic pump. *J. Gen. Physiol.* **57**:125–163.

STEVENS, C. F. 1964. A quantitative theory of neuronal interactions: theoretical and experimental investigations. Ph.D. Thesis. The Rockefeller University, New York.

TERZUOLO, C. A., and Y. WASHIZU. 1962. Relation between stimulus strength, generator potential and impulse frequency in stretch receptor of crustacea. *J. Neurophysiol.* **25**:56–66.

WASHIZU, Y., and C. A. TERZUOLO. 1966. Impulse activity in the crayfish stretch receptor neuron. *Arch. Ital. Biol.* **104**:181–194.